Helicity and Reconnection in the Solar Corona: Observations

Richard C. Canfield and Alexei A. Pevtsov

Department of Physics, Montana State University, Bozeman

Solar coronal magnetic fields are twisted on all observed spatial scales, though studies have emphasized active regions and their complexes. The overall twist of active region magnetic fields inferred from coronal images exhibits a hemispheric chirality preference. This twist has been shown to be consistent statistically with vector magnetic field observations in the photosphere, and is arguably of sub-photospheric origin. The manner in which active regions are observed to connect with one another through the corona implies that it is favorable, from the point of view of current closure and energetics, for active regions to reconnect with other of the same chirality. Transport of twist through reconnection from one coronal flux system to another has been observed in flares, jets, and large-scale eruptions, presumably associated with the shedding of helicity generated by the solar dynamo. Finally, X-ray observations show that structures that are significantly twisted are closely associated with coronal mass ejections.

1. INTRODUCTION

The striking coronal images from the the Soft X-ray Telescope [Tsuneta et al., 1991] on the Yohkoh mission [Ogawara et al., 1991] call attention to the topology of coronal magnetic fields. Figure 1 shows a striking equatorial array of S-shaped coronal structures within and between several bright active regions. We use the term sigmoidal [Rust and Kumar, 1996] to identify such structures of S or inverse-S form. Everywhere in the corona except within the negligible volumes of current sheets, the thermal/magnetic energy ratio β is small. Hence magnetic terms dominate over gravitational and pressure gradient terms in force balance, and the magnetic induction $\mathbf{B}$ satisfies the force-free field equation $\nabla \times \mathbf{B} = \alpha \mathbf{B}$. Sigmoidal structure can be quantified in this approximation, using α as a parameter.

Figure 1

Models of force-free fields can be compared to measurements of sigmoidal structures to infer values of α, as a measure of twist. Although force-free fields can be modeled quite generally from photospheric magnetogram data using sophisticated computational methods [Jiao et al., 1997; McClymont et al., 1997], these techniques are too demanding computationally to apply to large datasets. Two approximate models have been developed for the latter purpose.

Rust and Kumar [1996] modeled sigmoidal structures, in the force-free approximation, as helically kinked

flux ropes, shown in Figure 2. They measured the amplitude of the twist of the field lines by the ratio of the major radius R to the axial length of one turn of the helix L, which they parameterized by $k = 2\pi/L$. Values of both R and L can be derived from observations, taking care to avoid projection effects. In this model, α is related simply to R and the constant $x_0 = 2.4$, the first zero of the Bessel function of order 0, by $\alpha R = x_0$.

Figure 2

Pevtsov, Canfield and McClymont [1997] modeled the projection of three-dimensional constant-α force-free fields of a simple bipole, as shown in Figure 3. They used a two-dimensional force-free-field model to derive the relationship between the crossing angle γ that the central sigmoidal field lines make to the line joining the conjugate polarities, separated by distance L. In this model $\alpha = (\pi/L)\ \sin\ \gamma$.

Figure 3

Neither of these models [Rust and Kumar, 1996; Pevtsov et al., 1997] is sufficiently robust to be useful for quantitative studies, and future improvements on them would reward us with better understanding of the relationship between the structure of magnetic fields at various levels of the solar atmosphere, as well as their stability.

2. HEMISPHERIC CHIRALITY PREFERENCE

The lowest-order quantity that can be derived from the sigmoidal structures is the chirality, or handedness, of the helical structures that give rise to them. Rust and Kumar [1996] and Pevtsov and Canfield [1998] used Yohkoh SXT coronal X-ray images to identify sigmoidal structures. The results of these two studies are compared in Table 1. When divided along simple hemispheric lines, the two studies are consistent: 60 – 70% of such brightenings in the Northern hemisphere are of inverse-S form, and in the Southern hemisphere, of forward-S form. It is important for subsequent interpetation to note that the preference is weak; not all of the sigmoids in each hemisphere have the same chirality. It is also useful to think of a simple memory device: those shaped like the letter S occur in the South, and those shaped like an inverse-S, which look like the letter N, in the North. Figure 3 shows that S shapes correspond to positive α values.

Table 1

How is this hemispheric chirality rule related to that found in the photospheric magnetic fields of active regions [Pevtsov and Canfield, 1999]? Pevtsov, Canfield, and McClymont [1997] used a dataset of regions that had been observed both in the corona and in the photosphere. The coronal twist α_c was determined from the crossing angle γ. The photospheric twist α_p was determined from photospheric vector magnetograms. Fig-

ure 4 shows the measurements. The data set consists of only 44 active regions, since only they showed clear sigmoids, i.e. the angle γ was significantly non-zero; that is why there are no data points for small α_c values. The result is that such regions have the same sign of α in the photosphere and the corona in 39 of the 44 cases (90%), and the opposite sign in only 5 cases (10%). The reason for those of opposite sign is obvious when the images are examined in detail; both S and inverse-S structures are sometimes observed in a single active region.

Figure 4

Hα filaments in active regions [Rust, 1999] also show a hemispheric chirality rule, which is about as weak as that for coronal sigmoids in active regions. Ambiguities in the interpretation of the prominences images prevent a fully unambiguous inference of their chirality. If prominence material collects in concave-upward portions of coronal field lines, as is commonly believed, then prominences show the same hemispheric chirality rule as coronal loops do [Rust, 1999]. It would be very surprising if it were otherwise, given the largely force-free and therefore highly nonlocal nature of the magnetic field of the corona.

Twist has been studied in the corona on spatial scales larger than active regions, using Yohkoh SXT coronal images [Sandborgh et al., 1998] such as that in Figure 1. On the basis of the connections that can be seen in those images, [Sandborgh et al., 1998] determined the boundaries (separatrices) between flux systems. The sizes of these flux systems range up to tens of degrees in latitude and longitude; their lifetimes range up to five solar rotations. Some of these flux systems contain large-scale coronal loops of S or inverse-S shape that allow us to distinguish the chirality of their magnetic fields. Typically, the flux systems maintain their chirality throughout their lifetimes. They obey the same weak hemispheric chirality rule as active regions.

Systematic flows are present in the convection zone on variety of spatial scales [Kosovichev, 1999]. The same statement applies to turbulence. At the largest scales, there is now evidence for slow, long-lived cellular flows in the Sun's convection zone with typical diameters of tens of degrees and lifetimes of one or more rotations, both in magnetic fields [Ambroz, 1992] and the flows themselves [Beck et al., 1998; Hathaway et al., 1998]. This interpretation is supported by numerical simulations of convection and its interaction with magnetic flux [Brummell et al., 1996], which show large-scale coherent structures spanning the full vertical extent of the computational domain, involving multiple density scale heights (analogous to the full depth of the convection zone). The Sandborgh et al [1998] study of flux sys-

tems show that there is significant twist on comparable scales in space and time. At active region scales, there is evidence of turbulence in the twist of photospheric magnetic fields [Pevtsov and Canfield, 1999; Longcope, 1999], though the relationship between still smaller surface flows and those in the underlying convection zone is not as clear. In view of the presence of a hemispheric asymmetry, and the weakness of the hemispheric rule at and above active region scales, we expect future researchers to look at on the relationship between coronal structures and sub-photospheric flows on all these scales.

3. ROLE OF CURRENTS IN MAGNETIC RECONNECTION

As active regions rise into the corona from beneath the photosphere, they are initially isolated flux systems [Babcock, 1961]. In the corona they spread out and begin to reconnect with the surrounding flux. It has long been known that regions located in opposite hemispheres have opposite East – West orientation of their polarities [Hale et al., 1919]. This polarity law is evident in both magnetograms in Figure 5. This figure shows two contrasting examples. In the upper figure, the coronal image show obvious connections between regions in opposite hemispheres. In the lower figure, they do not. Canfield, Pevtsov, and McClymont [1996] studied the chirality of these active regions, and 25 other pairs, using photospheric vector magnetograms. They found a clear tendency for regions to connect preferentially with others of the same chirality .

Figure 5

There is an interesting difference between the explanations advanced for this observation and that advanced to explain reconnection in laboratory spheromak plasmas [Ji, 1999]. In the latter, reconnection proceeds more rapidly in the counter-helicity case, and this is attributed to the fact that the the anti-parallel components of **B** at the current sheet separating the current systems are greater. In the case of the solar observation, the anti-parallel components are not much different in the co-helicity and counter-helicity cases, since the fields are always rather close to potential, and as well, this explanation does not fit the observations.

Current conservation arguments have been advanced that do fit the trans-equatorial reconnection observation [Canfield et al., 1996]. The argument is illustrated in Figure 6. Consider the photospheric footpoints of the pair of active regions as shown in Figure 6a. The pair on the left is the co-helicity case, the pair on the right, counter-helicity. Figure 6b shows that reconnection of the co-helicity bipoles along the paths indicated does

Figure 6

not require a change of the currents at the footpoints, whereas the counter-helicity case, where the question marks appear, does require a change. This is a problem if the currents are imposed from below and continuity is required through the photosphere.

Energetics arguments have been advanced to explain reconnection in solar flares, and they, too, may fit the trans-equatorial reconnection observation [Melrose, 1997]. Figure 7 shows a schematic diagram of current-carrying loops before (light) and after (dark) reconnection. The case shown is one of several modeled, but does not have quite the same geometry as the trans-equatorial observation. The general requirement of the model is that the reconnecting structures have the same flux and current at the footpoints before and after reconnection. Hence, the model allows reconnection only between loops of the same chirality – the co-helicity case. Melrose [1997] shows that co-helicity reconnections are preferred on energetics grounds.

Figure 7

Neither of the existing explanations are sufficiently complete or relevant to be compelling explanations of the observations. In particular, the validity of the assumption of unchanging current and the flux threading the photosphere needs investigation.

4. TWIST AND RECONNECTION IN PRE-ERUPTIVE STRUCTURES

Many solar observations imply that twist is found in magnetic structures that show a tendency to erupt. In an observational study of 28 solar prominences that showed helical patterns, Vrsnak, Ruzdjak, and Rompolt [1991] found that eruptive prominences show higher observed twist than quiet ones. Furthermore, no observed prominence had a value of twist greater than 2π. Rust and Kumar [1996] studied large coronal transient brightenings of the type known to be associated with filament eruptions and coronal mass ejections. These brightenings are predominantly sigmoidal. Figure 8 shows that if their twist is measured as discussed in Section 1, the distribution drops off abruptly below $kR = 0.6$, the threshold for the $m = 1$ kink mode [Rust and Kumar, 1996].

Figure 8

Twist may build up in a given flux system through shear motions [van Ballegooijen, 1999] and/or through reconnection, e.g. [Van Ballegooijen and Martens, 1990]. However, it is the propagation of twist from one flux system in the photosphere to another in the corona that is particularly interesting in view of the Sun's need to get rid of all of the twist that is created in the solar dynamo [Bieber and Rust, 1995].

An example in which reconnection and transfer of

twist to larger scales (inverse-cascading) seems to play a role before an eruption is shown in Figure 9 [Pevtsov et al., 1996]. In the first two frames of the figure, one sees what appear to be two separate structures shaped like fish hooks. The arrow in panel (b) shows the gap between them. Later, in panels (c) through (e), the gap seems to be bridged and a single inverse-S sigmoidal loop seems to be present. The region erupted between the times of panels (e) and (f). The conclusion of the authors is that after reconnection the total twist in the coronal part of the sigmoid exceeded the threshold for the kink instability [Priest, 1984], which led to eruption. It must be noted, though, that one must not take too simplistic a view of the role of the kink mode; the Aly-Sturrock theorem [Aly, 1991; Sturrock, 1991; Antiochos, 1998]. places strong requirements on the magnetic field topology, and simple kinking is not the whole story.

Figure 9

Another example of reconnection and transfer of twist to larger scales prior to eruption was observed before a famous Yohkoh flare [Canfield and Reardon, 1998]. In an MPEG movie on CDROM in the referenced publication, several preflare events can be seen in which twist is observed to propagate from an emerging flux system into a pre-existing filament, which subsequently erupts. A schematic diagram intended to explain these events in terms of the transfer of twist between flux system is shown in Figure 10, which shows two loops, a twisted one connecting A to B; and an untwisted one connecting C to D. After reconnection, a larger loop is formed from A to D and a shorter one from C to B. Just after the moment of reconnection, all of the twist in the longer A – D loop is concentrated in only part of its length, and it spreads as a twist packet until it reaches equilibrium. What seen in the observations is the propagation of a spinning cylindrical region from an emerging flux system, indicated by what is called an arch filament, to the filament flux system. Initially the filament flux system responds by simply undulating; after several such episodes of twist propagation, the filament erupts.

Figure 10

We close by noting recent observational work that links sigmoidal structures to coronal eruptions and their effects on Earth. We know from earlier work discussed above [Rust and Kumar, 1996] that transient sigmoidal structures are associated with eruptions. In particular, sigmoidal brightenings have recently been observed prior to so-called halo CMEs, i.e., coronal mass ejections directed toward Earth [Sterling and Hudson, 1997; Hudson et al., 1998]. The implication of that finding is that improved ability to predict solar eruptions that will have an effect on space surrounding Earth will

result from improved understanding of the relationship between the topology of coronal structures and their eruption.

Acknowledgments. This research has been supported by NASA through SR&T grant NAG5-5043 and the Yohkoh Soft X-Ray Telescope contract NAS8-40801.

REFERENCES

Aly, J. J., How much energy can be stored in a three-dimensional force-free magnetic field?, *Astrophys. J., 375*, L61–L64, 1991.

Ambroz, P., About the Large-Scale Turbulent Transport of Magnetic Field, in Harvey, K. L. (Ed.), *The Solar Cycle*, pp. 35–43, Conference Series, Vol. 27, Astronomical Society of the Pacific 1992.

Antiochos, S. K., The Magnetic Topology of Solar Eruptions, *Astrophys. J., 502*, L181–+, 1998.

Babcock, H., The Topology of the Sun's Magnetic Field and the 22-Year Cycle, *Astrophys. J., 304*, 542–559, 1961.

Beck, J. G., Duvall, T. L., Scherrer, P. H., and Hoeksema, J. T., The Detection of Giant Velocity Cells on the Sun, *Eos Trans. AGU, 79*(17), S281, 1998.

Bieber, J. W. and Rust, D. M., The Escape of Magnetic Flux from the Sun, *Astrophys. J., 453*, 911+, 1995.

Brummell, N. H., Hurlburt, N. E., and Toomre, J., Turbulent Compressible Convection with Rotation. I. Flow Structure and Evolution, *Astrophys. J., 473*, 494+, 1996.

Canfield, R. C., Pevtsov, A. A., and McClymont, A. N., Magnetic Chirality and Coronal Reconnection, in Bentley, R. D. and Mariska, J. T. (Eds.), *Magnetic Reconnection in the Solar Atmosphere*, pp. 341–346, Proceedings of a Yohkoh Conference, Astronomical Society of the Pacific 1996.

Canfield, R. C. and Reardon, K. P., The Eruptive Flare of 15 November 1991: Preflare Phenomena, *Sol. Phys., in press* 1998.

Hale, G. E., Ellerman, F., Nicholson, S. B., and Joy, A. H., The Fields of Force in the Atmosphere of the Sun, *Astrophys. J., 49*, 153, 1919.

Hathaway, D. H., Bogart, R. S., and Beck, J. G., A Search for Giant Cells on the Sun, *Eos Trans. AGU, 79*(17), S281, 1998.

Hudson, H. S., Lemen, J. R., St. Cyr, O. C., Sterling, A. C., and Webb, D. F., X-Ray Coronal Changes during Halo CMEs, *Geophys. Res. Lett., tbd*, tbd–+, 1998.

Ji, H., Laboratory Studies of Magnetic Reconnection and Magnetic Helicity, in Brown, M. R., Canfield, R. C., and Pevtsov, A. A. (Eds.), *Magnetic Helicity in Space and Laboratory Plasmas*, Geophys. Monogr. Ser., AGU, Wahington, D.C. 1999.

Jiao, L., McClymont, A. N., and Mikic, Z., Reconstruction of the Three-Dimensional Coronal Magnetic Field, *Sol. Phys., 174*, 311–327, 1997.

Kosovichev, A. G., Flows in the Convection Zone: SOHO SOI/MDI Results, in Brown, M. R., Canfield, R. C., and Pevtsov, A. A. (Eds.), *Magnetic Helicity in Space and Laboratory Plasmas*, Geophys. Monogr. Ser., AGU, Wahington, D.C. 1999.

Longcope, D. W., Twist in Rising Magnetic Flux Tubes, in

Brown, M. R., Canfield, R. C., and Pevtsov, A. A. (Eds.), *Magnetic Helicity in Space and Laboratory Plasmas*, Geophys. Monogr. Ser., AGU, Wahington, D.C. 1999.

McClymont, A. N., Jiao, L., and Mikic, Z., Problems and Progress in Computing Three-Dimensional Coronal Active Region Magnetic Fields from Boundary Data, *Sol. Phys., 174*, 191–218, 1997.

Melrose, D. B., A Solar Flare Model Based on Magnetic Reconnection between Current-carrying Loops, *Astrophys. J., 486*, 521+, 1997.

Ogawara, Y., Takano, T., Kato, T., Kosugi, T., Tsuneta, S., Watanabe, T., Kondo, I., and Uchida, Y., THE SOLAR-A MISSION - AN OVERVIEW, *Sol. Phys., 136*, 1+, 1991.

Pevtsov, A. A. and Canfield, R. C., Do Photospheric Motions Cause Sheared Coronal Loops?, *Eos Trans. AGU*, *79*(17), S273, 1998.

Pevtsov, A. A. and Canfield, R. C., Helicity of the Photospheric Magnetic Field, in Brown, M. R., Canfield, R. C., and Pevtsov, A. A. (Eds.), *Magnetic Helicity in Space and Laboratory Plasmas*, Geophys. Monogr. Ser., AGU, Wahington, D.C. 1999.

Pevtsov, A. A., Canfield, R. C., and McClymont, A. N., On the Subphotospheric Origin of Coronal Electric Currents, *Astrophys. J., 481*, 973, 1997.

Pevtsov, A. A., Canfield, R. C., and Zirin, H., Reconnection and Helicity in a Solar Flare, *Astrophys. J., 473*, 533, 1996.

Priest, E. R., Solar magneto-hydrodynamics, in *Geophysics and Astrophysics Monographs, Dordrecht: Reidel, 1984* 1984.

Rust, D. M., Magnetic Helicity in Solar Filaments and Coronal Mass Ejections, in Brown, M. R., Canfield, R. C., and Pevtsov, A. A. (Eds.), *Magnetic Helicity in Space and Laboratory Plasmas*, Geophys. Monogr. Ser., AGU, Wahington, D.C. 1999.

Rust, D. M. and Kumar, A., Evidence for Helically Kinked Magnetic Flux Ropes in Solar Eruptions, *Astrophys. J., 464*, L199–, 1996.

Sandborgh, S. C., Canfield, R. C., and Pevtsov, A. A., Chirality of Large-Scale Flux Systems in the Solar Corona, *Eos Trans. AGU*, *79*(17), S285, 1998.

Sterling, A. C. and Hudson, H. S., Yohkoh SXT Observations of X-Ray "Dimming" Associated with a Halo Coronal Mass Ejection, *Astrophys. J., 491*, L55–+, 1997.

Sturrock, P. A., Maximum energy of semi-infinite magnetic field configurations, *Astrophys. J., 380*, 655–659, 1991.

Tsuneta, S., Acton, L., Bruner, M., Lemen, J., Brown, W., Caravalho, R., Catura, R., Freeland, S., Jurcevich, B., and Owens, J., The soft X-ray telescope for the SOLAR-A mission, *Sol. Phys., 136*, 37–67, 1991.

van Ballegooijen, A. A., Photospheric Motions as a Source of Twist in the Photosphere and Corona, in Brown, M. R., Canfield, R. C., and Pevtsov, A. A. (Eds.), *Magnetic Helicity in Space and Laboratory Plasmas*, Geophys. Monogr. Ser., AGU, Wahington, D.C. 1999.

Van Ballegooijen, A. A. and Martens, P. C. H., Magnetic fields in quiescent prominences, *Astrophys. J., , 361*, 283–289, 1990.

Vrsnak, B., Ruzdjak, V., and Rompolt, B., Stability of prominences exposing helical-like patterns, *Sol. Phys., 136*, 151–167, 1991.

Richard C. Canfield and Alexei A. Pevtsov, Department of Physics, Montana State University, Bozeman, MT 59717-3840. (e-mail: canfield@physics.montana.edu)

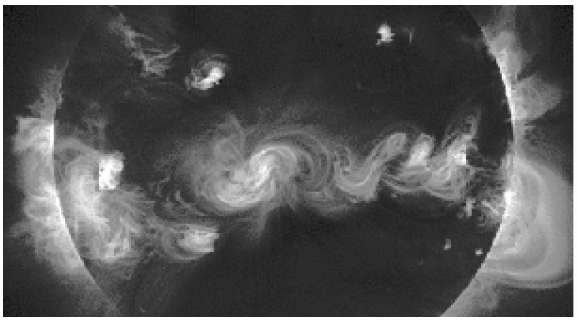

Figure 1. Yohkoh SXT X-ray image of the solar corona, showing magnetic flux systems and S-shaped sigmoidal structures within them. Such structures trace isolated magnetic field lines because thermal conduction along field lines is so much greater than that across it.

Figure 1. Yohkoh SXT X-ray image of the solar corona, showing magnetic flux systems and S-shaped sigmoidal structures within them. Such structures trace isolated magnetic field lines because thermal conduction along field lines is so much greater than that across it.

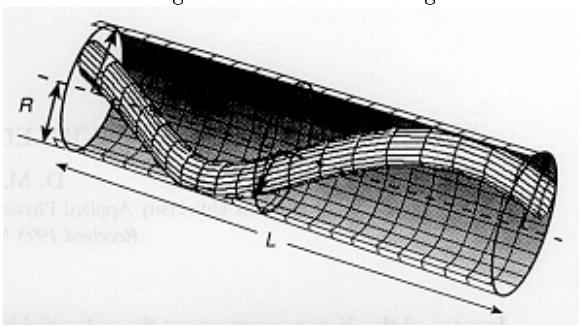

Figure 2. Model of a kinked ($m = 1mode$) flux rope used to quantify the sigmoidal shape of coronal structures. By permission [Rust and Kumar, 1996].

Figure 2. Model of a kinked ($m = 1mode$) flux rope used to quantify the sigmoidal shape of coronal structures. By permission [Rust and Kumar, 1996].

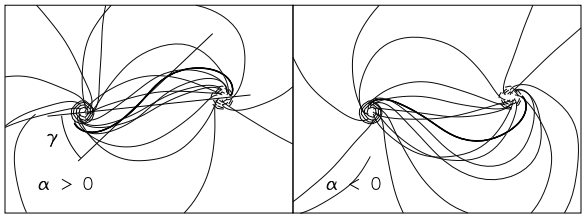

Figure 3. Model bipolar linear force-free field lines for positive and negative values of α. The heavy solid lines highlight low-lying sigmoidal field lines.

Figure 3. Model bipolar linear force-free field lines for positive and negative values of α. The heavy solid lines highlight low-lying sigmoidal field lines.

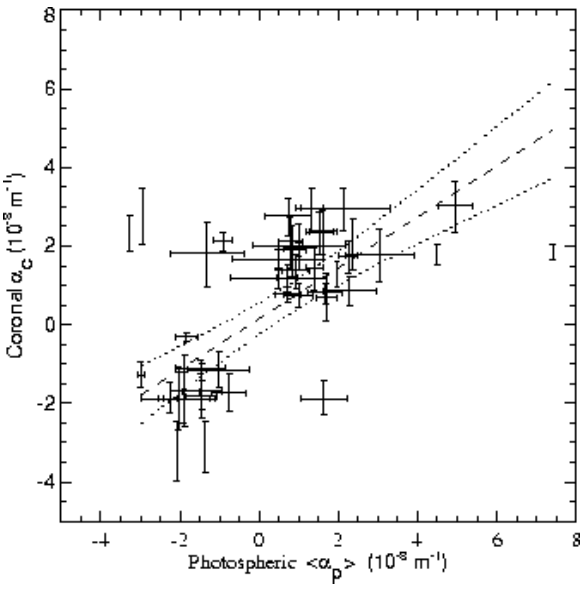

Figure 4. Observed force-free field parameter α from photospheric vector magnetograms (α_p) and from the geometry of coronal loops (α_c) for 44 active regions. Error bars show one standard deviations in both parameters. Error bars for α_c correspond to 10° standard deviation in the measured angle γ. Active regions without error bars in α_p are represented by only one magnetogram. The best linear fit (long dashed line) and 2 σ error band (short dashed lines) are shown.

Figure 4. Observed force-free field parameter α from photospheric vector magnetograms (α_p) and from the geometry of coronal loops (α_c) for 44 active regions. Error bars show one standard deviations in both parameters. Error bars for α_c correspond to 10° standard deviation in the measured angle γ. Active regions without error bars in α_p are represented by only one magnetogram. The best linear fit (long dashed line) and 2 σ error band (short dashed lines) are shown.

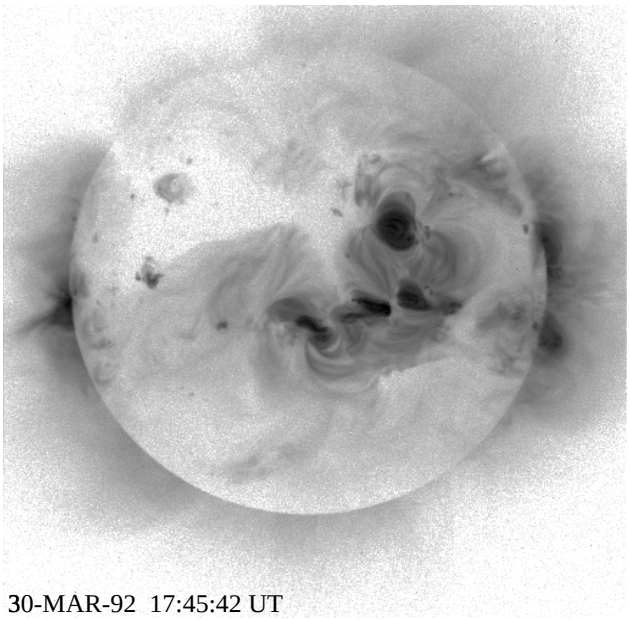

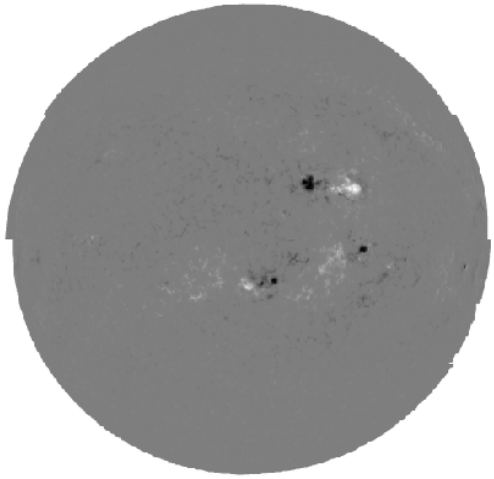

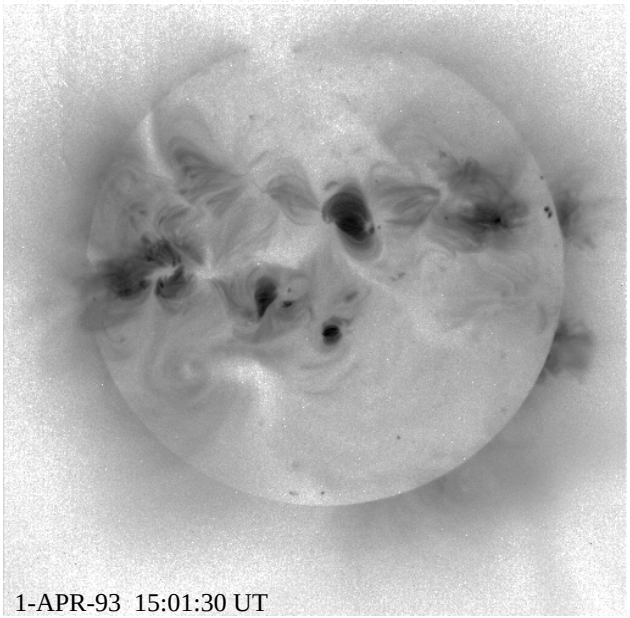

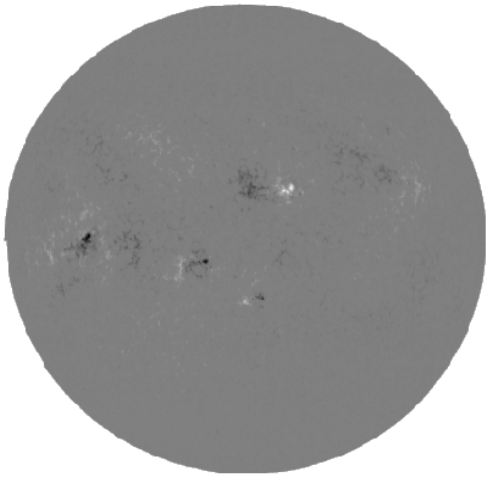

Figure 5. Coronal X-ray image (negative) and line-of-sight photospheric magnetic field map (white indicates magnetic field pointed into the Sun) showing a well-connected trans-equatorial pair of regions, which have the same chirality (top) and a poorly-connected trans-equatorial pair of regions, which have opposite chirality.

Figure 5. Coronal X-ray image (negative) and line-of-sight photospheric magnetic field map (white indicates magnetic field pointed into the Sun) showing a well-connected trans-equatorial pair of regions, which have the same chirality (top) and a poorly-connected trans-equatorial pair of regions, which have opposite chirality.

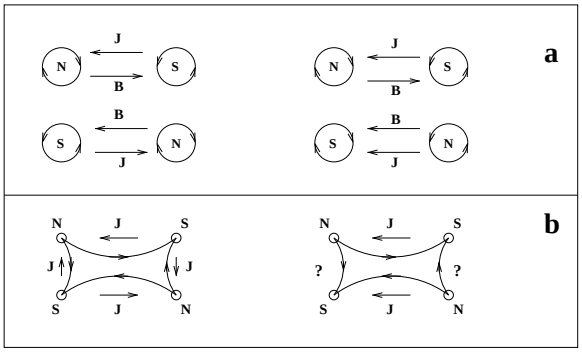

Figure 6. Diagram showing current closure argument for active regions in the co-helicity (left) and counter-helicity (right) cases. (a) Schematic representation, looking down on the photosphere, of the photospheric footpoints of two current-carrying flux tubes on opposite sides of the solar equator, before reconnection. Circles with arrows show the direction of the azimuthal component of the field. (b) Topology of the magnetic field lines and currents in the post-reconnection loops, viewed from above.

Figure 6. Diagram showing current closure argument for active regions in the co-helicity (left) and counter-helicity (right) cases. (a) Schematic representation, looking down on the photosphere, of the photospheric footpoints of two current-carrying flux tubes on opposite sides of the solar equator, before reconnection. Circles with arrows show the direction of the azimuthal component of the field. (b) Topology of the magnetic field lines and currents in the post-reconnection loops, viewed from above.

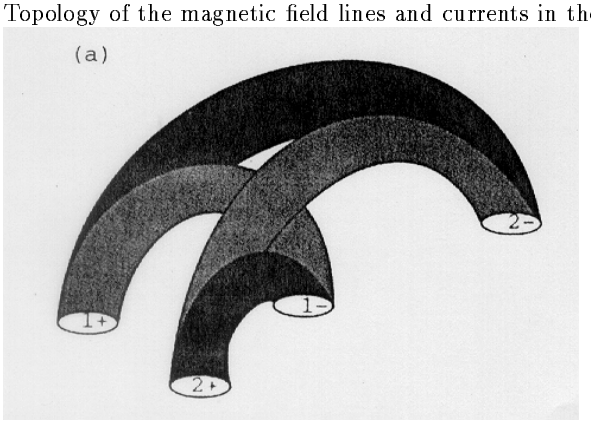

Figure 7. Schematic diagram showing loops before and after reconnection [Melrose, 1997]. Initially loops 1 and 2 (lightly shaded) connect footpoints 1+, 1- and 2+, 2-, respectively. The final loops (darkly shaded) connect footpoints 1+, 2- and 2+, 1- respectively.

Figure 7. Schematic diagram showing loops before and after reconnection [Melrose, 1997]. Initially loops 1 and 2 (lightly shaded) connect footpoints 1+, 1- and 2+, 2-, respectively. The final loops (darkly shaded) connect footpoints 1+, 2- and 2+, 1- respectively.

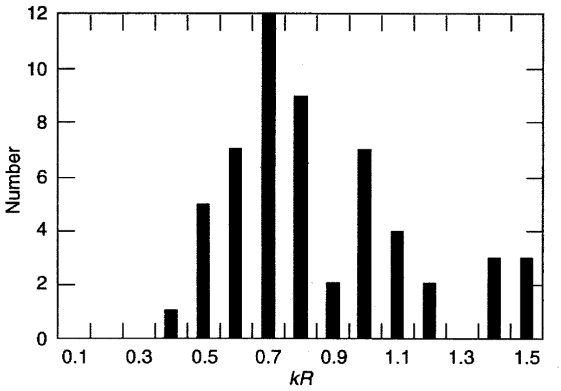

Figure 8. Distribution of sigmoid brightenings as a function of $kR = 2\pi R/L$. By permission [Rust and Kumar, 1996].

Figure 8. Distribution of sigmoid brightenings as a function of $kR = 2\pi R/L$. By permission [Rust and Kumar, 1996].

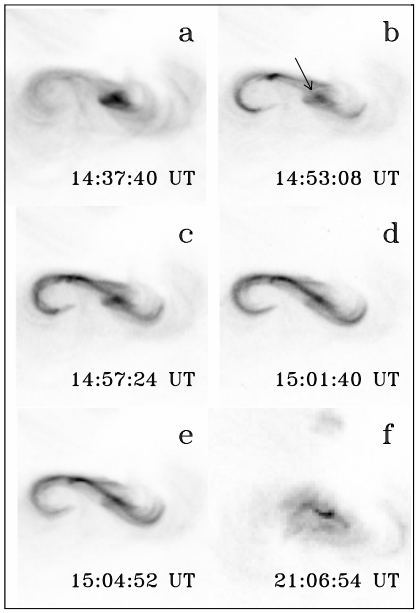

Figure 9. Sequence of Yohkoh SXT images showing the development of an inverse S loop before the flare of 1992 May 8 15:12 UT, between frames (e) and (f).

Figure 9. Sequence of Yohkoh SXT images showing the development of an inverse S loop before the flare of 1992 May 8 15:12 UT, between frames (e) and (f).

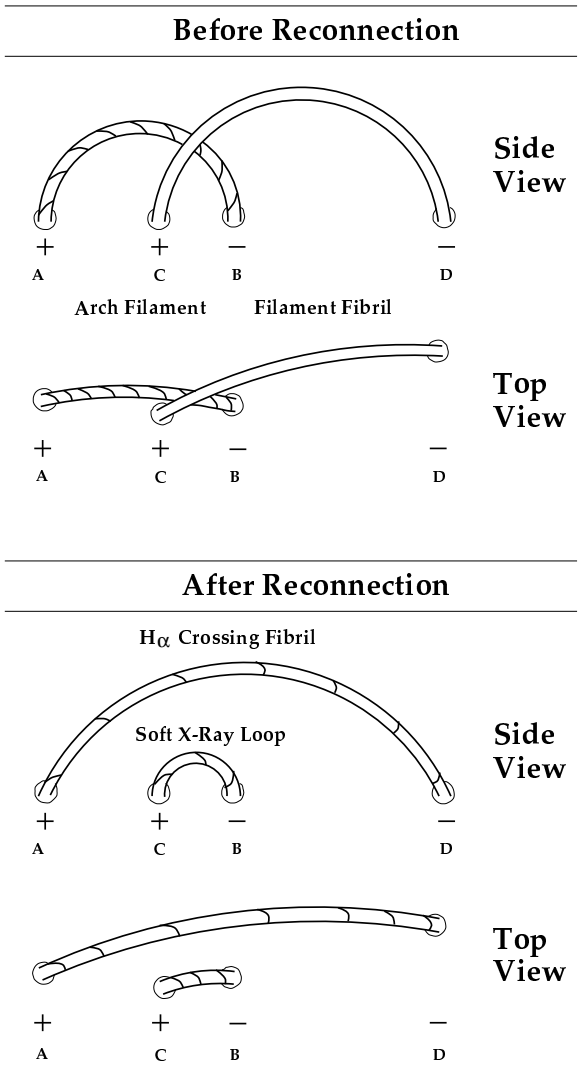

Figure 10. Cartoon model of the relationship between chromospheric structures (arch filaments, filament fibrils, and crossing fibrils) and the soft X-ray loops of the transient brightenings, before and after reconnection.

Figure 10. Cartoon model of the relationship between chromospheric structures (arch filaments, filament fibrils, and crossing fibrils) and the soft X-ray loops of the transient brightenings, before and after reconnection.

Table 1. Distribution of coronal sigmoids by hemisphere

	Forward S	Inverse S	Total
Rust and Kumar [1996]			
Northern	4	24	28
Southern	40	12	52
Cross-equator	12	11	23
Total	56	47	103
Pevtsov and Canfield [1998]			
Northern	32	47	79
Southern	70	33	103
Total	102	80	182

HELICITY AND RECONNECTION IN THE SOLAR CORONA

CANFIELD AND PEVTSOV

HELICITY AND RECONNECTION IN THE SOLAR CORONA

CANFIELD AND PEVTSOV

HELICITY AND RECONNECTION IN THE SOLAR CORONA

CANFIELD AND PEVTSOV

HELICITY AND RECONNECTION IN THE SOLAR CORONA

CANFIELD AND PEVTSOV

HELICITY AND RECONNECTION IN THE SOLAR CORONA

CANFIELD AND PEVTSOV

HELICITY AND RECONNECTION IN THE SOLAR CORONA

CANFIELD AND PEVTSOV

HELICITY AND RECONNECTION IN THE SOLAR CORONA

CANFIELD AND PEVTSOV

HELICITY AND RECONNECTION IN THE SOLAR CORONA

CANFIELD AND PEVTSOV

HELICITY AND RECONNECTION IN THE SOLAR CORONA

CANFIELD AND PEVTSOV

HELICITY AND RECONNECTION IN THE SOLAR CORONA

CANFIELD AND PEVTSOV

HELICITY AND RECONNECTION IN THE SOLAR CORONA

CANFIELD AND PEVTSOV

HELICITY AND RECONNECTION IN THE SOLAR CORONA

CANFIELD AND PEVTSOV

HELICITY AND RECONNECTION IN THE SOLAR CORONA

CANFIELD AND PEVTSOV

HELICITY AND RECONNECTION IN THE SOLAR CORONA

CANFIELD AND PEVTSOV

HELICITY AND RECONNECTION IN THE SOLAR CORONA

CANFIELD AND PEVTSOV

HELICITY AND RECONNECTION IN THE SOLAR CORONA

CANFIELD AND PEVTSOV